Structure Formation via Polymer Demixing in Spin-Cast Films

Stefan Walheim, Martin Böltau, Jürgen Mlynek, Georg Krausch,† and Ullrich Steiner*

Fakultät für Physik, Universität Konstanz, 78457 Konstanz, FRG

Received December 31, 1996; Revised Manuscript Received April 3, 1997[⊗]

ABSTRACT: The domain structure in thin films of an immiscible polystyrene/poly(methyl methacrylate) (PS/PMMA) blend was studied after spin-casting from a common solvent. Atomic force microscopy (AFM) combined with selective dissolution was used to obtain three-dimensional information on the domain morphology in thin films. Three different common solvents and three different substrate surfaces were studied. Distinct differences in the thin film domain structure and surface topography are observed depending on the substrate surface energy and the solubility of the two polymers in the three solvents. The topographic modulation can be explained by a different rate of solvent evaporation during spin-coating for the two phases. The normal and lateral organization of the phase-separated domains is governed by a complex interplay between preferential aggregation of one phase at the substrate and phase segregation in the film. Additionally, some of the results suggest that a dewetting process may be involved in the domain formation. The structures obtained after spin-casting are far from thermodynamic equilibrium. The equilibration of the films during annealing depends strongly on the phase morphology, and long-lived metastable configurations are found.

Introduction

Bulk demixing of binary polymer mixtures have been studied extensively during the last decades and are reasonably well understood.[1−7] Near interfacial boundaries, however, surface effects may lead to physical properties that significantly differ from those in bulk.[8] In particular, the demixing process of a multicomponent blend is usually strongly influenced by the presence of an interface, which may lead to surface-oriented phase separation,[9] or the formation of a wetting layer.[10] Conversely, the presence of a surface field can induce the breakup of a surface layer, as shown in several studies concerning dewetting phenomena.[11,12] In thin films, the confinement of polymers between two surfaces is known to play a role in modifying parameters associated with the phase equilibria and the kinetics of phase segregation.[13,14] Most previous studies focused on demixing phenomena in polymer melts. In many practical applications, however, polymer films are prepared by a sudden extraction of a solvent. In semiconductor industry, for example, photoresist layers and dielectric coatings are usually prepared using the spin-coating technique. Due to the intrinsic immiscibility of most macromolecular blends, polymer mixtures typically demix during the rapid solvent-casting process. The resulting phase-separated morphology may be far from thermodynamic equilibrium, and relaxation toward equilibrium may be hindered by kinetic barriers formed by the nonequilibrium phase morphology.

An increasing availability of techniques with high lateral and depth resolution resulted in recent experimental studies on lateral structures formed by polymer demixing in thin films. Reich[15] has investigated polymer−polymer phase separation in rather thick films (several microns). Bruder and Brenn[16] and Straub *et al.*[17] examined the time development of lateral phase-separated domains in a thin, binary polymer film. Steiner *et al.*[18] observed the formation of lateral domains during the equilibration of a bilayer consisting of two immiscible polymers. Geoghean *et al.*[19] used nuclear reaction analysis, neutron reflectometry and transmission electron microscopy to study the phase morphology in thin polystyrene/polybutadiene films. Employing forward recoil spectrometry and optical microscopy, Krausch *et al.*[20] studied the lateral demixing of polystyrene and partially brominated polystyrene on a prestructured substrate. For diblock copolymers, Mayes *et al.* observed micro phase separation already after spin-casting[21] More recently, Affrossman *et al.*[22] and Tanaka *et al.*[23] investigated the domain morphology of an immiscible binary polymer blend spin-cast from toluene solution with atomic force microscopy. They find a marked topographic structure that accompanies the formation of lateral domains.

In the present work, we try to gain a better understanding of the phase morphology of a thin film after the rapid solvent evaporation that occurs during the spin-coating process. As a model system, we studied symmetric blends of polystyrene (PS) and poly(methyl methacrylate) (PMMA). This mixture has been studied before, in terms of both its bulk demixing properties,[24] and the PS and PMMA phase behaviors in thin layers.[23] Particularly in the thin film configuration, a rich variety of features have been observed that differ from those known from the bulk demixing processes. The present work studies the same system, but several additional issues are investigated in order to gain a better insight into the complex processes that take place during the spin-coating procedure: (a) the origin of the topographic structure and its dependence on the spin-casting solvent; (b) the role of the substrate surface in the formation of the domain structures; (c) the evolution of the spin-cast structures toward thermodynamic equilibrium.

Experimental Section

Materials. The polymers used in this work were polystyrene (PS) and poly(methyl methacrylate) (PMMA), purchased from Polymer Standards Service and used as obtained. Their characteristics are listed in Table 1. Solvents for spin-coating were analytic grade toluene, tetrahydrofuran (THF) (stabilized

* To whom correspondence should be addressed. Tel: +49-7531-883824. Fax: +49-7531-883072. E-mail: ulli.steiner@uni-konstanz.de.

† Present address: Institut für Physikalische Chemie, Ludwig Maximilians Universität München, Theresienstrasse 39, 80333 München, FRG.

⊗ Abstract published in *Advance ACS Abstracts,* July 15, 1997.

S0024-9297(96)01928-6 CCC: $14.00

Table 1. Characteristics of PS and PMMA

polymer	M_w	M_w/M_n
PS	94 900	1.06
PMMA	100 000	1.05

Table 2. Characteristics of Substrate Surfaces

substrate	surface treatment	static water contact angle[a] (deg)
silicon oxide	snow-jet	0
gold	directly after evaporation	65
ODM		108

[a] ±3°.

with 250 mg/L 2,6-di-*tert*-butyl-4-methylphenol) and methyl ethyl ketone (MEK). Polymer films were prepared by the spin-coating technique from a PS/PMMA (50/50 w/w) solution (typically 3% of polymer by weight) in one of the three solvents. The film thickness was controlled by varying the rotation speed. The average film thickness ranged from 70 to 140 nm. Macroscopic examination of the polymer films after spin-coating revealed smooth, slightly opaque films. The higher volatility of THF and MEK, when compared to toluene, caused a radial thickness variation of the films,[25] but in all cases the lateral length scales of the thickness variation were much larger than the size of the domains. Sample annealing was carried out in a vacuum oven (1×10^{-5} mbar) at 190 ± 1 °C.

Surface Preparation. The substrates used in the experiments were highly polished silicon wafers, whose surfaces were treated in three different ways in order to modify their surface energies. As a high-energy surface, the native oxide layer of the silicon substrate was used. Organic residues on the silicon oxide surface were removed by cleaning the silicon wafer under a jet of CO_2-ice crystals ("snow-jet").[26] To produce surfaces with intermediate surface energies, first a 2 nm thick chrome layer was evaporated onto the silicon substrate, followed by the deposition of a 50 nm thick gold layer. To avoid contamination, the substrates were used immediately after the gold deposition. To produce low-energy surfaces, a self-assembled alkane monolayer was deposited onto the substrate surfaces by immersing gold-covered silicon wafers overnight in a 0.285% (w/w) solution of octadecylmercaptan (ODM) in an ethanol/THF mixture (5/2 w/w). Since no experiment was available to quantitatively measure the substrate surface energies, we used the static water contact angle to qualitatively characterize the substrates.[27] The contact angles of the surfaces used in this study, silicon oxide (SiO_x), gold (Au), and organic monolayer (ODM), are summarized in Table 2. We note that a large variation of the static water contact angle was observed depending on the details of the surface manipulation. Cleaning the SiO_x surface using the snow-jet technique resulted in a reduction of the water contact angle from 30 to 0°. Gold surfaces measured directly after the evaporation process exhibited a water contact angle of 65°, which increased to 80° after storing the gold-covered wafers for several days under ambient conditions. Both effects are attributed to the adsorption of organic molecules onto the high-energy surfaces. Similarly, water contact angles ranging from 100 to 110° are obtained on the ODM surface, depending on the quality of the gold surface prior to immersion in the ODM solution. In spite of these possible contamination effects, the substrate surface characteristics summarized in Table 2 could be reproducibly obtained.

Atomic Force Microscopy. For topographic imaging, a Park Scientific atomic force microscope (AFM) and a home-built "stand-alone" AFM were used. All experiments (except for the swelling experiment in the next section) were performed in contact mode. Information on the polymer distribution inside the film can be obtained by removing one of the two phases using a selective solvent for this polymer.[12] First several scalpel scratches were applied to the samples, the AFM tip was aligned with respect to a characteristic feature (e.g., an intersection of two scratches) using an optical microscope, and the samples were imaged by the AFM. In this image the height difference between the substrate surface exposed by the scratch and the polymer layer yields the film thickness. Then, the polymer phase that covered most of the air surface was dissolved with a selective solvent that only slightly alters the other phase. The sample was immersed for 5 min in either cyclohexane to remove the PS, or in acetic acid to dissolve the PMMA-rich phase. After drying, the samples were again aligned under the AFM tip as described above, and an AFM picture of the identical surface area was taken. Cross-sections of the two topography images were superimposed to yield the information on the polymer composition profile inside the sample.

While this procedure overcomes the limitation of the AFM, which in its standard mode yields only surface information, special care has to be taken to avoid artifacts generated during exposure of the sample to the selective solvents. Such artifacts include the removal of small, insoluble domains that may be "washed away" by the solvent or a modification of the phase boundaries by an increased polymer mobility in the insoluble domains. Also, a very thin layer of either phase that may cover the free surface of the entire sample may not withstand the selective solvent treatment. To investigate the effect of selective solvents on the phase conformation at the sample surface, we studied the surface composition of one sample with an AFM operated in the elasticity mode.[28] In the this mode, the tip is held in contact with the surface and the normal load (5 nN) applied to the cantilever is vibrated at a frequency of 7.5 kHz and a peak-to-peak amplitude of 0.6 nm perpendicular to the sample surface. Phase sensitive detection of the cantilever bending yields a measure for the tip indentation that is determined by the local elasticity of the surface. Due to a difference in the elastic moduli, this technique enables us to distinguish between PS and PMMA.[29,30] Both the topographic and elasticity images can be obtained in a single scan. Figure 1a shows the topographic AFM image of a PS/PMMA sample spin-cast from toluene solution onto a silicon oxide surface. In Figure 1b the corresponding elasticity image is displayed. The topography image exhibits elevated islands that lie some 30 nm above a lower surface level. The elasticity image reveals that the composition of the islands differs from the surrounding surface. A reduced vibration amplitude at the round domains indicates a higher local stiffness of the islands. Removal of the PS layer with cyclohexane enables the unambiguous assignment of the elasticity response to the polymer distribution at the surface. The image in Figure 1c shows the same features as in Figure 1a, but the height difference between the "islands" and the lower lying level has increased to some 50 nm. The corresponding elasticity image reveals no contrast between the PS and PMMA plateaus. A comparison of Figure 1a,c allows us to assign the PMMA-rich phase to the "islands" (bright) surrounded by a PS-rich phase (dark). Also, a comparison of Figure 1a,c shows that even the smallest details discernible in Figure 1a are still present after the cyclohexane treatment (Figure 1c). The remaining PMMA phase exhibits sharp edges whose widths (~50 nm) are limited by the pyramidal shape of the AFM tip. The comparison in Figure 1 verifies the soundness of our experimental approach, and since the selective solvent procedure provides the quasi three-dimensional polymer composition information in the film, this approach is adopted for most measurements described in the present article.

In some experiments, samples were exposed to a solvent vapor during the AFM scan. Since solvent swollen polymer films are too soft to allow contact-mode AFM, tapping mode AFM, was used to image the surface topography.[31] In tapping mode AFM, a cantilever with a spring constant of 40 N/m is vibrated at its resonance frequency (~280 kHz). As the vibrating tip approaches the surface, the oscillation is damped, and the AFM feedback mechanism can be locked at a given amplitude damping. In the tapping mode, the AFM images the topography of the sample surface without applying a mechanical load, which makes this imaging mode suitable for soft or liquid surfaces.

Results and Discussion

Surface Morphology. We start our discussion with the domain structures found on a Au substrate after

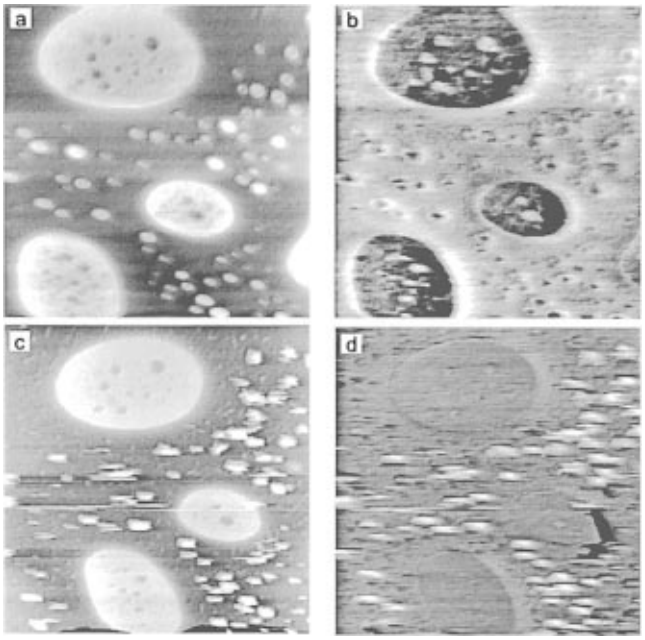

Figure 1. AFM images (7.5 × 7.5 μm) of a 70 nm thick PS/PMMA film on a silicon oxide surface. The sample was prepared by spin-casting from toluene. The topographic image (a) and the elasticity mode image (b) were obtained in a single scan. The elasticity contrast in (b) reveals a difference in the composition makeup of the elevated "islands" (a) compared to the lower lying phase. In (c) and (d), the PS phase was removed with cylohexane, and the topographic image (c) shows unchanged PMMA-rich islands on top of a continuous PMMA layer that covers the silicon oxide surface. The corresponding elasticity image (d) shows no contrast. Except for artifacts caused by the AFM tip, all details in (a) and (b) are reproduced in (c), indicating that the cyclohexane treatment leaves the PMMA-rich phase essentially unchanged. The lower quality of (c) and (d) is caused by the several times repeated scans of the same area, which were necessary to find the same scan area as in (a) and (b).

spin-casting a PS/PMMA film from three different solvents (Figure 2). Following the spin-casting of the polymer film onto a gold surface, all three samples reveal a characteristic laterally phase-separated morphology of PS- and PMMA-rich domains. In addition to the formation of lateral domains of different polymer composition, all samples exhibit a topographical structure that coincides with the polymer phases. To further investigate the samples, the PS-rich phase was removed by immersing the sample in cyclohexane for 5 min, and an AFM picture of the identical area was taken to reveal the surface structure of the remaining PMMA phase. Figure 2a−c shows a sample spin-cast from toluene. The AFM image exhibits a continuous, interconnected PMMA structure that is elevated by some 40 nm from the PS background phase. The plateau-like PMMA domains display well-defined sharp edges and a steep decline to the surrounding PS rich phase. The dark areas at the top-left corner of the AFM images display the bare Au substrate after removal of the polymer film by a scalpel scratch. A cross-section (Figure 2c) through the film before (Figure 2a) and after (Figure 2b) dissolving the PS reveals that both the PS and the PMMA phases extend from the gold to the air surface, with well-defined apparent interfaces of a width of some 100 nm. We note that the AFM images were taken with an AFM tip with a 71° apex angle. Since the measured width of sharp, high steps are limited by the tip geometry, the step widths measured here are entirely determined by the tip. The two polymers are strongly incompatible, and the interfacial width that separates the PS-rich and PMMA-rich phases is expected to be a few nanometers.[32] In Figure 2d−f a sample was similarly spin-cast from a THF solution. The morphology of the phases is similar to Figure 2a−c, with a PMMA structure that exhibits connected "islands" rather than a continuous structure. Here, the topography contrast is reduced compared to Figure 2a−c, with the PMMA islands protruding only 20 nm from the PS background. In addition an approximately 30 nm thick continuous PMMA layer has formed at the Au surface. A dramatic change occurs if MEK is employed as common solvent in the sample preparation procedure (Figure 2g−i). Here, isolated PS islands protrude from a PMMA background. In contrast to Figure 2a−c where the protruding structures feature sharp edges, the PS islands in Figure 2g−i form a round, droplike topographical structure.

To gain insight into the formation of the topographic structure of the domains, the model in Figure 3 is put forward. Initially, PS, PMMA, and the solvent mix and the solute drop that is put onto the substrate at the beginning of the spin-coating process form a single phase (Figure 3a). During the spin-coating process, the solvent evaporates and coexisting PS-rich and PMMA-rich phases form, both of which still contain solvent (Figure 3b). At this intermediate point, where the phases are still liquid due to their solvent content, the sample surface is essentially flat due to the small difference in surface tension of the two phases. Even though the solvents used are common solvents for both polymers, the relative solubilities of the two polymers in these solvents vary. Toluene is a better solvent for PS than for PMMA; therefore, at each moment during spin-coating, the PS-rich phase contains more toluene than the PMMA phase. As more solvent evaporates, a characteristic time is passed where there is practically no toluene left in the PMMA phase, while the other phase is still swollen with toluene. Further evaporation collapses the swollen PS phase to a level that lies much below the interface of the higher PMMA structures (Figure 3c). Inversely, MEK preferentially dissolves PMMA and accumulates in the PMMA-rich phase, which leads to protruding PS domains (Figure 3d).

A necessary ingredient of our model in Figure 3 is a different solubility of PS and PMMA in the three solvents investigated. Since published data on the solubility of polymers in solvents is scarce, we perform several qualitative experiments to check the solubility of PS and PMMA in toluene, THF, and MEK. We do this by investigating the inverse process—the swelling of PS and PMMA when exposed to the vapor of the three different solvents. The degree of swelling was observed by the change in interference colors after pure PS and PMMA films were introduced into a vapor atmosphere. In the case of toluene, PS exhibited a much stronger swelling compared to a PMMA film. For THF, the degree of swelling was similar for the two samples with PS exhibiting a slightly larger thickness increase compared to PMMA. The effect was inverted when the two samples were brought into a MEK atmosphere, with PMMA showing a stronger swelling response than PS.

To further corroborate the model proposed above, we prepared a sample similar to the one in Figure 1a and investigated its swelling in a solvent atmosphere. Since solvent-swollen polymer films are too soft to allow contact mode AFM, tapping mode AFM was used to image the surface topography. In Figure 4a we show a tapping mode image of a PS/PMMA sample spun from

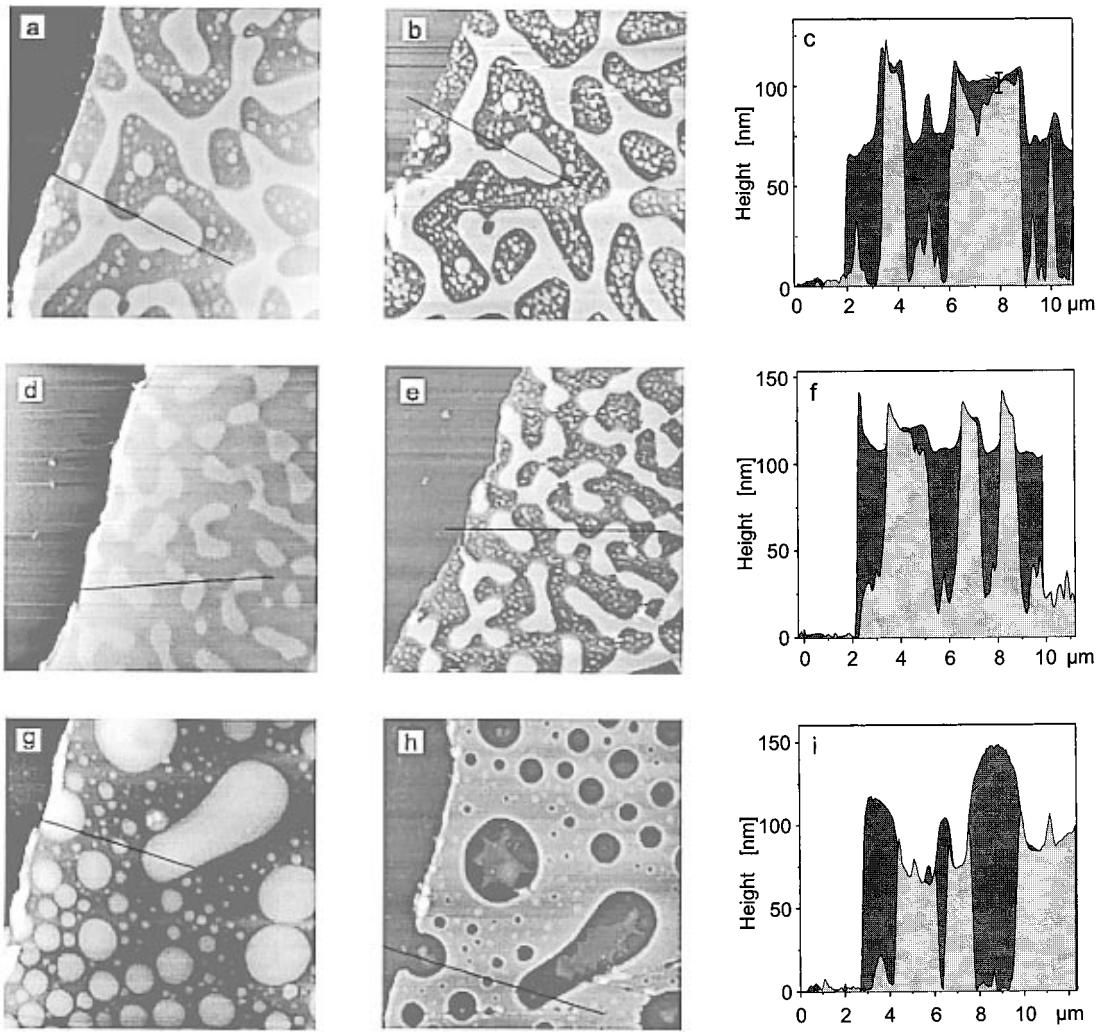

Figure 2. AFM images (14 × 14 μm) of PS/PMMA mixtures spin-cast from three different solvents onto a Au surface: (a)−(c) toluene; (d)−(f) THF; (g)−(h) MEK. The first column (a, d, g) contains topographic images of the PS/PMMA samples as cast. In the second column (b, e, h) the PS-rich phase was removed by immersion in cyclohexane, and the AFM images display the remaining PMMA surface. In the third column (c, f, i), cross-sections of the topographic images before and after cyclohexane immersion were superimposed to show the vertical PS and PMMA distribution (PS, dark gray; PMMA, light gray). The error bar in (c) indicates the accuracy of the superposition procedure. The lines in topographic images (a, d, g and b, e, h) indicate the locations where the cross-sections were taken. The origin of the topographic variation of the PS/PMMA domains lies in the varying solubility of PS and PMMA in their three common solvents. Toluene and THF are better solvents for PS, and thus PMMA is more quickly depleted of the solvent during the spin-coating process. This leads to elevated PMMA structures (bright regions in (a) and (d)). The opposite effect is observed in the case of MEK, which is a better solvent for PMMA, and PS islands (bright) are observed after spin-coating (g).

toluene solution. Tapping mode AFM yields the same topographic information as the contact mode, as can be seen from a comparison of Figure 4a and Figure 1a (taken with contact mode AFM). In Figure 4b, the sample and the AFM tip were brought into a toluene atmosphere. Compared to Figure 4a, the topographic contrast is inverted, with the PS phase elevated above the PMMA domains that formed the elevated structures in Figure 4a. The swelling of the sample by toluene affects the PS-rich phase more rapidly and to a higher extent than the PMMA phase. Once the sample is removed from the toluene vapor, the topographic contrast reverts to the original state (Figure 4c).

In a similar study, Tanaka *et al.*[23] propose an alternative explanation for the height variation of the PS/PMMA phase-separated morphology in thin films after spin-coating. In their model, they describe a lateral spreading mechanism of the PS-rich phase that displaces the PMMA-rich phase normal to the film surface. In our present study, we find no evidence for the contribution of such a mechanism to the formation of the topographic modulation of the film surface.

Substrate Dependence of the Phase Morphology. In thin films, the phase separation of the two polymers during the spin-coating process is necessarily influenced by the presence of the two interfaces. To systematically examine the role of the substrate surface, substrates of different surface energies were employed. Three substrate surfaces were used in this study: silicon oxide (SiO_x), gold (Au), and an organic monolayer (ODM) on a gold-covered surface (Table 2).

In Figure 5, films of PS/PMMA mixtures spin-cast from THF are shown on the two different substrate surfaces: SiO_x (Figure 5a−c) and ODM (Figure 5d−f). In addition, the phase morphology of PS/PMMA from THF on a Au surface (intermediate surface energy) is shown in Figure 2d−f. On the polar SiO_x surface (Figure 5a−c), the more polar PMMA forms a homogeneous 20−30 nm thick layer on the substrate. On top of this continuous layer, a characteristic phase-segregated domain structure is formed. Only little is changed, when the SiO_x wafer is replaced by a Au surface[33] (Figure 2d−f).

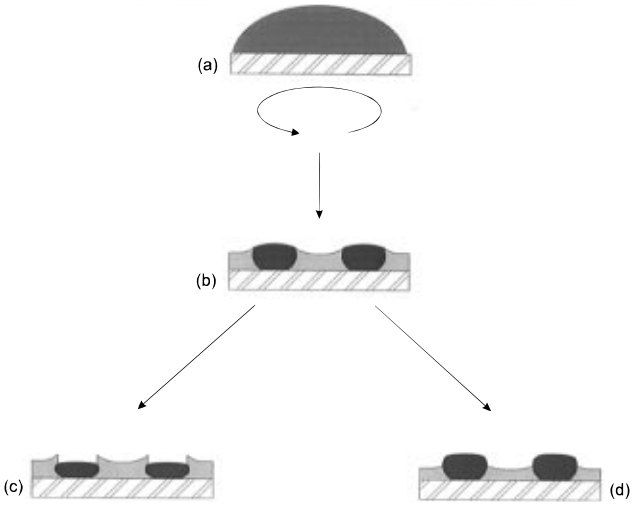

Figure 3. Schematic model describing the formation of the topographic structure during the spin-coating process. Initially, PS and PMMA are dissolved in a common solvent (a). During spin-coating, solvent evaporates and demixing of PS and PMMA sets in (b). At this stage, the sample surface is essentially smooth, apart from a small variation of the liquid surface caused by the different surface tensions of the PS- and PMMA-rich phases. Depending on the relative solubility of the two polymers in their common solvent, one of the phases is more quickly depleted of the solvent and turns solid earlier than the other phase. Subsequent evaporation of the remaining solvents leads to a further collapse of the better soluble phase. Toluene or THF are better solvents for PS, and the PS phase (dark gray) collapses below the average height of the PMMA layer (light gray) (c). For MEK, the PS-rich phase solidifies first, leading to elevated PS islands (d). The shape of the domains is determined by the different surface tensions of the two phases in (b): the phase with the lower surface tension (PS-rich) has a convex curvature in (b), as opposed to a concave surface structure of the PMMA phase. This leads to sharp edges of the PMMA domains in (c) as opposed to a more round topography in (d).

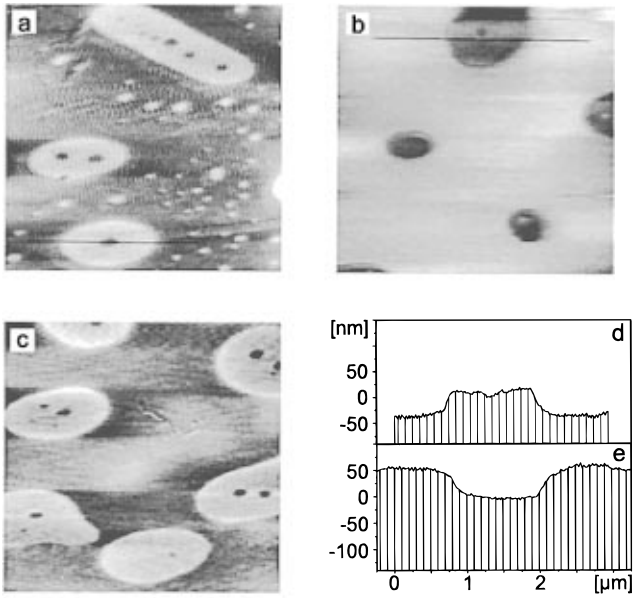

Figure 4. Tapping mode AFM pictures (3.6 μm × 3.6 μm) of PS/PMMA mixtures spin-cast from a toluene solution onto a silicon oxide layer. Initially, the 70 nm thick film exhibits elevated PMMA domains (bright) protruding from the PS background (dark) (a). In (b) the sample is exposed to toluene vapor during the AFM scan. Here the topographic contrast is inverted, due to the stronger swelling of the PS-rich phase (bright). After removal of the sample from the toluene vapor, the sample reverts to the original state (c). The cross-sections in (d) and (e) are taken from (a) and (b), respectively (solid lines in (a) and (b)), and show the relative height (normalized to the location of the PMMA/air surface).

A striking change in the polymer distribution occurs when PS/PMMA are spin-cast from THF onto a hydrophobic surface. This is shown in Figure 5d−f for a PS/PMMA blend spin-cast onto an ODM-covered substrate. The sample surface is more homogeneous than in Figure 5a, punctuated by isolated "holes". In contrast to the situation described above, selective dissolution experiments reveal that the almost homogeneous top layer consists mainly of PMMA rather than PS. In particular, the top layer is removed by selective dissolution of the samples in acetic acid, a selective solvent for PMMA. After dissolution, a continuous PS underlayer is revealed on the substrate surface (Figure 5e). Even though PS has a lower surface tension than PMMA, it is almost completely excluded from the air surface. In a similar experiment in Figure 6, a complete PS/PMMA bilayer was found on the entire sample surface after spin-coating from a THF solution onto an ODM surface, but the surface structure in Figure 5d proved to be the more common case. We attribute the difference between Figures 5d and 6 to fine differences between the ODM surfaces (possibly due to fine differences in the roughness and/or the thickness of the underlying Au film).

These results confirm earlier studies on the adsorption kinetics of a binary polymer melt near a substrate surface. Krausch *et al.*[34] and Kim *et al.*[35] have shown that by suitably choosing the substrate surface, a preferential adsorption of either phase at this surface can be obtained. Remarkably and in contrast to these earlier studies where only the phase next to the substrate surface was changed with varying surface energies, we observe a complete phase inversion from Figure 5a−c to Figure 5d−f. In Figures 5d−f and 6, the polymer with the higher surface tension (PMMA) almost completely covers the air surface. We note that the PMMA/PS bilayer in Figure 6 is far from equilibrium. An equilibration process would lead not only to a breakup of the PMMA surface layer but also to a dewetting of both, the PS- and PMMA-rich phases from the ODM substrate, as can be deduced from the wetting properties of PS and PMMA films on hydrocarbon surfaces.[12]

Figure 5 also indicates that by suitably selecting the substrate surface and spin-casting solvent, either polymer phase can be made to selectively adsorb at the substrate surface. While homogeneous layers can be observed next to the substrate surface, the phase adjacent to the air surface is usually disordered.

Formation of the Surface Structures. Even in the case of a monocomponent melt, films formed by the spin-coating process are not necessarily in thermal equilibrium.[36] This is even more so for a multicomponent mixture, where phase separation occurs during the spin-coating process. This is most clearly illustrated by Figure 2a, where the elevated PMMA structure exhibits sharp, slightly upwards turned edges. Unfortunately, the evolution of the phase morphology cannot easily be observed during the spin-coating process, and we must attempt to infer information about the mechanism of structure formation from the frozen-in structures after the solid film has formed. Most laterally segregated structures in Figures 2 and 5 bear strong resemblance to the late stages of bulk phase separation in a binary liquid mixture. In the absence of strong surface forces, which dominate the phase segregation process in thin

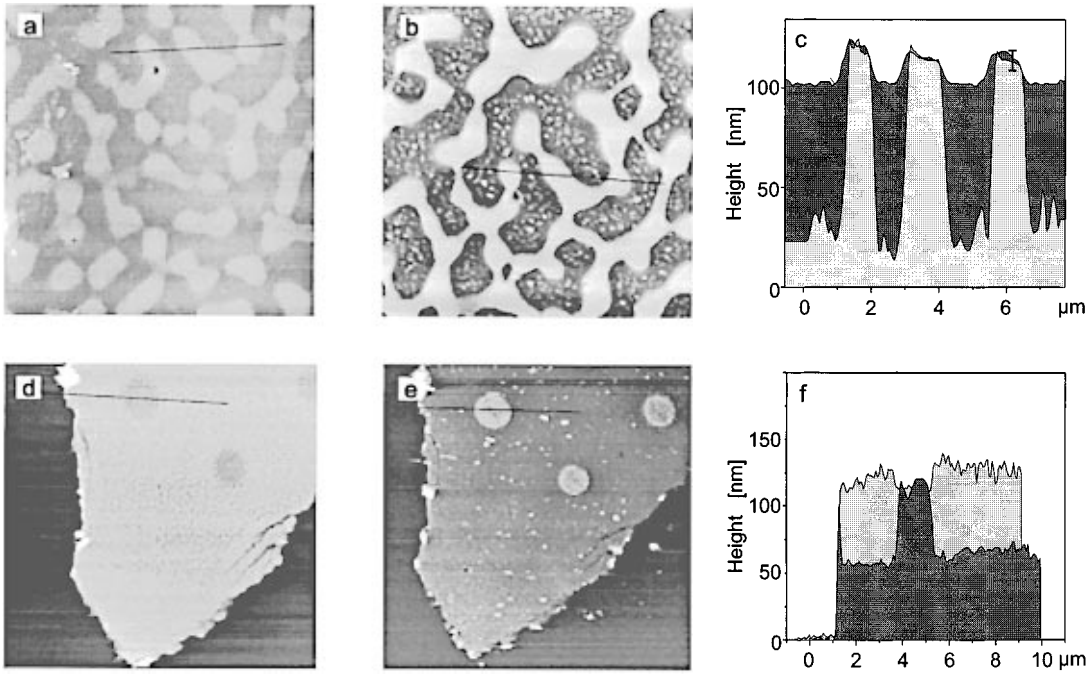

Figure 5. Substrate dependence of the PS/PMMA domain structure spin-cast from THF: (a−c) on SiO_x; (d−f) on ODM. The AFM pictures have lateral dimensions of 14 μm × 14 μm: (a, d) as spin-cast; (b) after immersion in cyclohexane to remove PS; (e) after immersion in acetic acid to remove the PMMA-rich phase. The cross-sections (c, f; lines in (a), (b), (d), (e)) reveal the vertical distribution of the PS (dark gray) and PMMA (light gray) phases (the error bar in (c) indicates the accuracy of the superposition procedure). PMMA preferentially adsorbs on the more polar SiO_x surface to form a homogeneous layer next to the substrate. On the ODM a PS/PMMA bilayer is observed, with PS next to the substrate. The PMMA layer (bright) is punctured by holes that are partially filled by the PS-rich phase (dark).

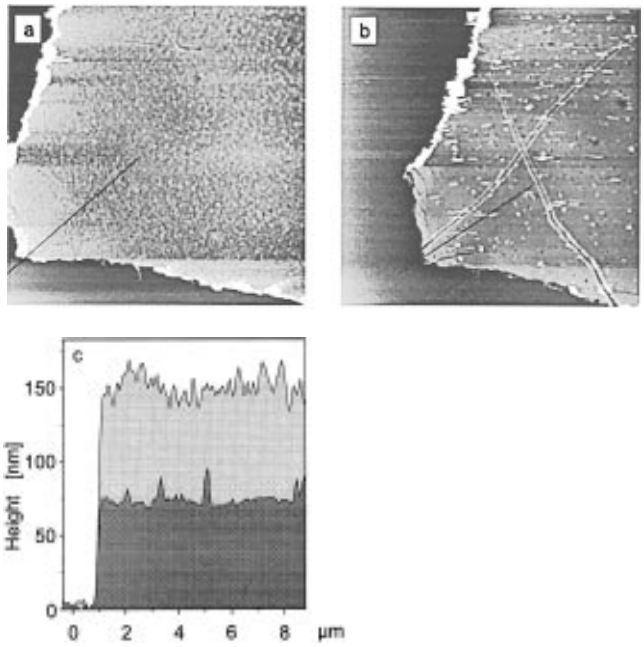

Figure 6. AFM images (17 × 17 μm) of PS/PMMA mixtures spin-cast from THF onto a ODM surface: (a) as spin-cast; (b) after immersion in acetic acid for 5 min, (c) cross-section taken at the position indicated by solid lines in (a) and (b). This sample is prepared in a way similar to that for the film shown in Figure 5(d−f), but here the film is homogeneous over the entire sample area. The number of holes in the PMMA surface film (light gray) (Figure 5d−f) depends sensitively on the details of the substrate surface treatment. The long diagonal scratches are caused by the coarse positioning of the AFM tip in the attempt to find the same scan area as in (a).

films, a demixing sample undergoes a bulk-type spinodal decomposition. Domains start growing in three dimensions until their sizes reach the thickness of the film, which itself decreases as a function of time during solvent evaporation. From then on, further growth is limited by the geometrical constraint of the film. Finally, the films become glassy, and the size of the lateral domains is determined by the complex interplay between the rapid quench and the continuously decreasing mobility, both caused by solvent evaporation. A domain formation that is primarily driven by a bulk-type phase separation process seems to be confirmed by Figure 7. Here films of varying overall film thickness were prepared from a toluene solution onto a Au surface. With decreasing film thickness from 140 nm in Figure 7a to 80 nm in Figure 7d, the characteristic size of the phase-separated domains decreases, but the four images seem to exhibit a self-similar domain structure. As confirmed by a qualitative observation of the spin-casting process, films of a larger film thickness (as controlled by the rotation speed of the spin-coater) take longer to dry, allowing for longer diffusion times and a higher degree of domain-coarsening during the spin-coating procedure. The resulting increase in lateral domain size is compatible with the assumption of a spinodal decomposition process of a binary mixture with subsequent domain growth, constrained to a quasi-two-dimensional configuration by the thickness of the film. A detailed analysis of Figure 7 indicates that the growth of domain size proceeds significantly faster than a linear relation. A more quantitative comparison of the increase of domain size with time, generated in a spin-coating process, is difficult, since the interplay of different parameters of the spin-coating process is not known.

Apart from an apparent resemblance of the phase-separated structures to bulk demixing in some of the samples, there are also indications for a second possible process of domain formation. The continuous PMMA layers (Figure 5a−c) and PS layers (Figure 5d−f) that cover the substrate indicate that at least some of the

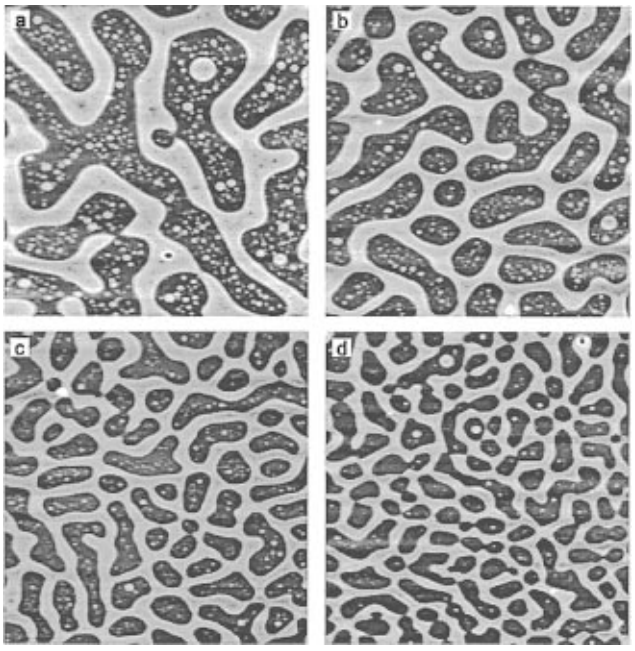

Figure 7. Film thickness series of the PS/PMMA mixture spin-cast from a toluene solution onto a Au surface. The average film thickness was varied by adjusting the rotation speed of the spin-coater from 2000 to 10000 rpm: (a) 140 nm; (b) 105 nm; (c) 95 nm; (d) 80 nm. While there is no change in the domain morphology (the PMMA domains (bright) protrude from the PS phase (dark)), the average domain size decreases from ~6 μm in (a) to ~2.5 μm in (d). The AFM image sizes are 28 μm (h) × 26 μm (w).

segregation process proceeds in a surface-oriented fashion. A comparison of Figures 5d and 6a suggests a possible dewetting process in a late stage of phase segregation. In the cases where one of the polymer phases shows a strong substrate preference, the initial phase separation may take place in a surface-oriented fashion, forming a transient bilayer.[17] As more solvent is evaporated from the film, the upper layer becomes unstable and holes are formed, which are filled by the lower liquid phase. Figure 5d could be interpreted as the early stage of such a hole formation process. As the holes grow and coalesce, either large drops (Figure 2g) or an interconnected structure are formed (Figure 2a,d). Note the qualitative difference between Figure 5a where complete lateral segregation is observed and Figure 5d where relatively isolated domains puncture an otherwise homogeneous bilayer. This morphological difference can be linked to a much higher stability of a bilayer where PS is covered by a PMMA film, as compared to PS on PMMA where rapid dewetting takes place.[37]

A closer look at the cross-sections of Figure 2 provides some additional information on a transient stage of the thin film structure, just before the complete drying process described above leads to the marked topography. The sketches in Figure 3 illustrate a possible mechanism that leads to the difference between the sharp-edged contours in Figure 2a and the round drops in Figure 2g. If neither of the two phases completely wets the air surface, the PS-rich phase assumes a convex curvature due to the lower surface tension of PS compared to PMMA, while the PMMA surface is concave near the PS/PMMA contact line[12] (Figure 3b). For spin-coating from toluene, the PS phase collapses, leaving the surrounding PMMA phase with sharp, slightly upward turned edge contours (Figure 3c). With MEK as a solvent, the PMMA phase collapses, leaving the round-shaped PS domains protruding from the surface (Figure 3d).

A further structural feature is noticeable in Figures 2 and 5. In addition to the large domain-like structures discussed above, much smaller domains can be detected inside both phases. We attribute these small domains to the deep quench during rapid solvent evaporation. During the spin-coating process, more and more solvent evaporates, and both phases are increasingly depleted of their minority component. Initially, the polymers in both phases retain a sufficient mobility to diffuse over the several micron large distances that separate the different phases. At very low solvent concentrations, the polymer diffusion coefficients are reduced to a value where the mass transport over the increasingly large distances can no longer take place, and in a secondary spinodal process, the small domains are formed.

While the present data are not sufficient to fully describe the domain formation during the spin-coating process with time, characteristic features in the frozen-in composition distributions of the samples indicate that competing surface-oriented and surface independent phase separation processes play a role, with the dominance of either process depending mainly on the surface energy of the chosen substrate.

Thermal Equilibration of the Surface Structures. Already a qualitative examination of Figures 2 and 4 suggests that the structures formed during the spin-coating process are not in thermodynamic equilibrium. In particular, the sharp edges of the elevated structures seem to defy the polymer surface tension. If the sample is prepared from toluene or THF, the phase with the higher polymer−air surface tension (PMMA) forms the islands or elevated terraces, while in thermodynamic equilibrium, the lower surface tension material (PS) is expected to form drops that protrude from the surface.[27] To test the stability of the structures found in the previous samples, we carried out two annealing series. In Figure 8, the surface domains of a PS/PMMA sample spun from toluene onto a SiO_x substrate are shown for increasing annealing times at $T = 190 \pm 1$ °C. Already after 5 min (Figure 8b), the topographic structure after spin-coating (Figure 8a) has inverted. The originally elevated PMMA islands in Figure 8a are transformed into depressions, and the PS phase forms interconnected round ridges. The lateral domain structure, on the other hand, has changed only a little from Figure 8a to Figure 8b. After an annealing time of 40 min, the continuous PS phase has formed separate domains that start to take the shape of drop-like conformations. After an annealing time of 12 h, the equilibrium configuration is reached, exhibiting spherical PS drops that protrude from a PMMA matrix. Further annealing does not change the domain morphology.

When the PS/PMMA film is prepared from a toluene solution onto a Au surface, a quite different development with annealing time is seen. Here, the unannealed structure features a continuous, elevated PMMA interconnected structure (Figure 9a). After an annealing time of 12 h, after which the PS/PMMA mixture on a SiO_x substrate has reached an equilibrium configuration (Figure 8d), the domain structure on a Au surface has changed only very little from its unannealed configuration (Figure 9b). The PMMA ridges have assumed a round curvature at the air surface, but no noticeable coarsening of the structure has taken place. Surprisingly, even after this long annealing time, the polymer

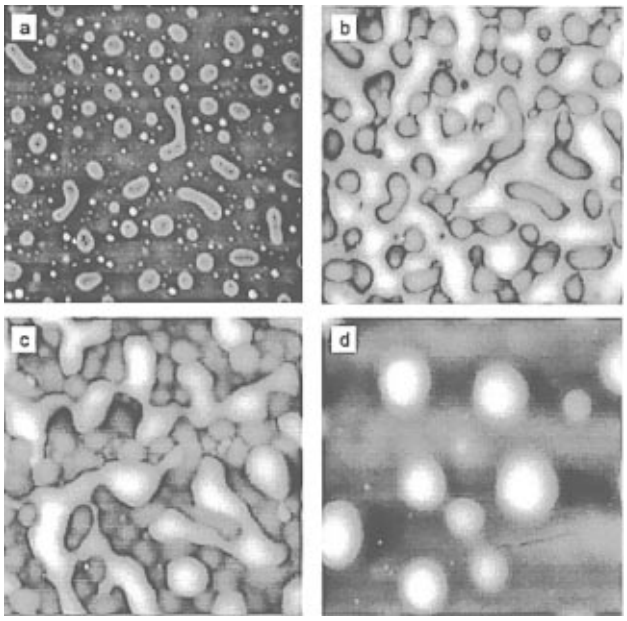

Figure 8. Annealing series (T = 190 °C) of the PS/PMMA domains on a SiO_x surface. The film (~70 nm thick) as cast from toluene exhibits PMMA islands (bright) protruding from a PS background (dark) (a). After an annealing time of 5 min (b), the topographic structure has inverted with the continuous PS structure (bright) elevated above the PMMA phase (dark). After 40 min (c), the PS domains have coarsened into partially connected drops, and after 12 h, the equilibrium configuration of PS drops suspended in a PMMA film is reached (d). The AFM image sizes are 17 μm × 17 μm. All four images were taken on the identical sample area.

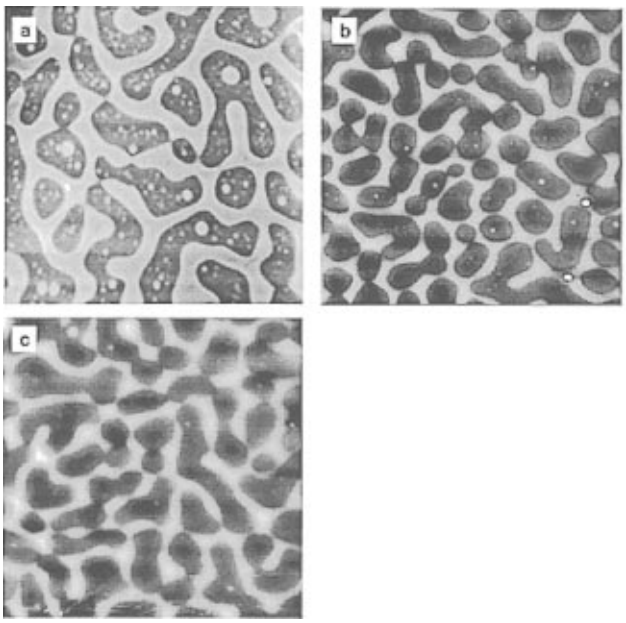

Figure 9. Annealing series of the PS/PMMA phase-separated domains on a Au surface. The film (~80 nm thick) as cast from toluene (a) exhibits a continuous PMMA structure (bright) that separates depressed PS domains (dark). After annealing for 12 h at 190 °C (b), the surface morphology has changed only slightly, with a rounding off of the sharp domain edges from (a). A longer annealing time (41 h at 190 °C in (c)) does not strongly change the PS/PMMA surface structure, though some accumulation of PMMA in the junctions of the interconnected domain structure is observed. The AFM image sizes are 17 μm × 17 μm. The three images were taken on different sample areas.

with the higher surface tension, PMMA, is still elevated above the PS-rich domains. After an annealing time of 41 h (Figure 9c), only little further development is seen, with some accumulation of PMMA in the junctions where the PMMA ridges meet. Since this phase morphology in Figure 9 changes only little with time, a long-lived metastable configuration must have been reached for this system during the spin-coating process.

While we presently lack a full explanation for the development of the phase morphology in Figure 9 with time, we note the main differences between Figures 8a and 9a. In Figure 8a, the disordered topographic structure lies on top of a homogeneous PMMA layer, whereas in Figure 9a the PS and PMMA domains straddle the entire film (see Figure 2c). Secondly, the PS-rich background phase in Figure 8a is interconnected, while the PS domains in Figure 9a are isolated from each other. These two observations determine the flow and diffusion mechanisms during the annealing process. In Figure 8a, the material transport in both phases can occur isotropically in the plane of the film by convective flow, until at a late stage the PS phase breaks up into isolated drops. In Figure 9, the PMMA mass transport can occur only along the ridges of the PMMA network. A lateral transport of the PS-rich phase can occur only by diffusion through the PMMA-rich phase, a process that is known to be very slow. In the absence of a fast mechanism for lateral PS diffusion, the only way for the system to form a structure with an elevated PS phase involves a lateral spreading of the interconnected PMMA ridges, a process that apparently is not favored at the gold surface. While it is unlikely that the domain structure in Figure 9c is in thermal equilibrium—the ridge structure should decay via a Rayleigh instability—the evolution toward equilibrium seems to be very slow due to constraints in the lateral material transport.

Conclusions

Spin-coating a film of strongly immiscible polymers from a common solvent yields lateral domains that exhibit a well-defined topographical structure (islands and plateaus) with sharp edges. These structures, which are far from their thermodynamic equilibrium, are essentially determined by two experimental parameters: (a) the different solubilities of the two polymers in their common solvent and (b) the varying substrate preferences of the two polymers. Two main features emerge from this study. If the common solvent is a better solvent for the polymer that has the lower surface tension, the topographical surface structure exhibits sharp, well-defined edges. In the opposite case, rather round surface structures are observed. Our experimental findings on the surface variations of thin spin-cast PS/PMMA films are in disagreement with a model proposed in an earlier study on the same system by Tanaka *et al.*[23] When the substrate surfaces are varied, homogeneous layers of either polymer phase next to the substrate can be observed. These two observations could lead to an application where surface-directed demixing of a multicomponent polymer mixture could be used to transfer a pattern on a microscopic or nanoscopic length scale into a composition variation of a polymer film.

Acknowledgment. This work was partially supported by the Volkswagen Stiftung and the Deutsche Forschungsgesellschaft (DFG) (Sonderforschungsbereich SFB 513, B2). U.S. acknowledges financial support

by a research fellowship (Habilitations-Stipendium) of the DFG.

References and Notes

(1) Binder, K. In *Materials Science and Technology*; Haasen, P., Eds.; VCH-Verlag: Weinheim, 1990; Vol. 5.
(2) de Gennes, P. G. *J. Chem. Phys.* **1980**, *72*, 4756.
(3) Pincus, P. *J. Chem. Phys.* **1981**, *75*, 1996.
(4) Lifshitz, I. M.; Slyozov, V. V. *J. Chem. Phys. Solids* **1961**, *19*, 35.
(5) Siggia, E. D. *Phys. Rev. A* **1979**, *20*, 595.
(6) Bates, F. S.; Wiltzius, P. *J. Chem. Phys.* **1989**, *91*, 3258.
(7) Schwahn, D.; Hahn, K.; Streib, J.; Springer, T. *J. Chem. Phys.* **1990**, *93*, 8383.
(8) Krausch, G. *Mater. Sci. Eng.* **1995**, *R14*, 1.
(9) Jones, R. A. L.; Norton, L. J.; Kramer, E. J.; Bates, F. S.; Wiltzius, P. *Phys. Rev. Lett.* **1991**, *66*, 1326.
(10) Steiner, U.; Klein, J.; Eiser, E.; Budkowski, A.; Fetters, L. J. *Science* **1992**, *258*, 1126.
(11) Reiter, G. *Phys. Rev. Lett.* **1992**, *68*, 75.
(12) Lambooy, P.; Phelan, K. C.; Haugg, O.; Krausch, G. *Phys. Rev. Lett.* **1996**, *76*, 1110.
(13) Reich, S.; Cohen, Y. *J. Polym. Sci., Polym. Phys. Ed.* **1981**, *19*, 1255.
(14) Neserov, A.; Horichko, V.; Lipatov, Y. *Macromol. Chem. Rapid Commun.* **1991**, *12*, 571.
(15) Reich, S. In *Soft Order in Physical Systems*; Rabin, Y., Bruinsma, R., Eds.; Plenum Press: New York; 1994; p 73.
(16) Bruder, F.; Brenn, R. *Phys. Rev. Lett.* **1992**, *69*, 624.
(17) Straub, W.; Bruder, F.; Brenn, R.; Krausch, G.; Bielefeldt, H.; Kirsch, A.; Marti, O.; Mlynek, J.; Marco, J. F. *Europhys. Lett.* **1995**, *29*, 353.
(18) Steiner, U.; Klein, J.; Fetters, L. *Phys. Rev. Lett.* **1994**, *72*, 1498.
(19) Geoghegan, M.; Jones, R. A. L.; Payne, R. S.; Sakellariou, P.; Clough, A. S.; Penfold, J. *Polymer* **1994**, *35*, 2019.
(20) Krausch, G.; Kramer, E. J.; Rafailovich, M. H.; Sokolov, J. *Appl. Phys. Lett.* **1994**, *64*, 2655.
(21) Mayes, A. M.; Russell, T. P.; Bassereau, P.; Baker, S. M.; Smith, G. S. *Macromolecules* **1994**, *27*, 749.
(22) Affrossman, S.; Henn, G.; O'Neill, S. A.; Pethrick, R. A.; Stamm, M. *Macromolecules* **1996**, *29*, 5010.
(23) Tanaka, K.; Takahara, A.; Kajiyama, T. *Macromolecules* **1996**, *29*, 3232.
(24) Kessler, J.; Higashida, N.; Shimomai, K.; Inoue, T.; Ougizawa, T. *Macromolecules* **1994**, *27*, 2448.
(25) Spangler, L. L.; Torkelson, J. M.; Royal, J. S. *Polym. Eng. Sci.* **1990**, *30*, 644.
(26) Sherman, R.; Hirt, D.; Vane, R. *J. Vac. Sci. Technol.* **1994**, *12*, 1876.
(27) Young, T. *Philos. Trans. R. Soc. London* **1805**, *95*, 65.
(28) Maivald, P.; Butt, H. J.; Gould, S. A. C.; Prater, C. B.; Drake, B.; Gurley, J.A.; Elings, V. B.; Hansma, P. K. *Nanotechnology* **1991**, *2*, 103.
(29) Krausch, G.; Hipp, M.; Böltau, M.; Marti, O.; Mlynek, J. *Macromolecules* **1995**, *28*, 260.
(30) The static indentation of the AFM tip into the PS domains is approximately 5 nm, compared to less than 1 nm in the case of PMMA, as measured by a comparison between contact mode and tapping mode AFM. The variation of the indentation depth due to the modulation is less than 0.6 nm. The molecular origin of the difference in local stiffness is not known, but the AFM elasticity experiment resembles macroscopic hardness (indentation) tests where PMMA is found to be harder (Rockwell hardness M80-M105) compared to PS (Rockwell hardness M65-M85).
(31) Zhong, Q.; Inniss, D.; Kjoller, K.; Elings, V. B. *Surf. Sci. Lett.* **1993**, *290*, L688.
(32) Russell, T. P.; Menelle, A.; Hamilton, W. A.; Smith, G. S.; Satija, S. K.; Majkrzak, C. F. *Macromolecules* **1991**, *24*, 5721.
(33) In this experiment we note a further solvent dependence of the polymer phase morphology. The homogeneous PMMA layer on the SiO_x and Au surfaces forms only after spin-coating from THF. For toluene and MEK, the lateral PS-rich and PMMA-rich domains extend almost entirely to the Au surface (Figure 2c,i). Only traces of PMMA between the PS domains and the respective substrate surface are left.
(34) Krausch, G.; Dai, C.-A.; Kramer, E. J.; Bates, F. S.; Marco, J. F.; Bates, F. S. *Macromolecules* **1993**, *26*, 5566.
(35) Kim, E.; Krausch, G.; Kramer, E. J.; Osby, J. O. *Macromolecules* **1994**, *27*, 5972.
(36) de Gennes, P. G. *C. R. Acad. Sci. Paris, Ser. II* **1988**, *307*, 1841.
(37) Reiter, G. Personal communication.

MA9619288